

## DC dielectrophoresis separation of marine algae and particles in a microfluidic chip

SONG YongXin<sup>1</sup>, YANG JianDong<sup>1</sup>, SHI XiaoFei<sup>4</sup>, JIANG Hai<sup>3</sup>, WU YanBin<sup>1</sup>, PENG Ran<sup>1</sup>,  
WANG Qi<sup>5</sup>, GONG Ning<sup>2</sup>, PAN XinXiang<sup>1</sup>, SUN YeQing<sup>2\*</sup> & LI DongQing<sup>1,3\*</sup>

<sup>1</sup>Department of Marine Engineering, Dalian Maritime University, Dalian 116026, China

<sup>2</sup>Institute of Environmental Systems Biology, Dalian Maritime University, Dalian 116026, China

<sup>3</sup>Department of Mechanical and Mechatronics Engineering, University of Waterloo, Waterloo, ON, N2L 3G1, Canada

<sup>4</sup>College of Information Science and Technology, Dalian Maritime University, Dalian 116026, China

<sup>5</sup>Department of Respiratory Medicine, the Second Hospital Affiliated to Dalian Medical University, Dalian 116026, China

Received November 8, 2011; accepted January 4, 2012; published online February 23, 2012

This paper reports a microfluidic method of continuous separation of marine algae and particles by DC dielectrophoresis. The locally non-uniform electric field is generated by an insulating PDMS triangle hurdle fabricated within a PDMS microchannel. Both the particles and algae are subject to negative DEP forces at the hurdle where the gradient of local electric-field strength is the strongest. The DEP force acting on the particle or the algae depends on particles' or algae's volume, shape and dielectric properties. Thus the moving particles and algae will be repelled to different streamlines when passing the hurdle. In this way, combined with the electroosmotic flow, continuous separation of algae of two different sizes, and continuous separation of polystyrene particles and algae with similar volume but different shape were achieved. This first demonstration of DC DEP separation of polystyrene particles and algae with similar sizes illustrates the great influence of dielectric properties on particle separation and potentials for sample pretreatment.

**DC dielectrophoresis, marine algae, particle, microfluidic chip, permittivity difference**

### 1 Introduction

Rapid analysis and characterization of bioparticles, such as cells, bacterial and microalgae become increasingly important in modern bioanalysis and also have wide application in environmental monitoring and water quality analysis [1]. For example, sensitive and fast determination of the types, sizes and concentration evolution of microalgae is an effective means for water quality monitoring and assessment [2]. For research in biology and bioengineering, it is essential to manipulate and separate randomly suspended microorganisms in a noninvasive manner. As regards to system biology, micro-separation plays the fundamental

role in understanding the connections of total elements and their dynamics over time [3].

In practice, however, the sample might be a composite mixture with both the target microorganisms and the impurities. Sometimes the size of the impurities is the same with that of the target microorganism. The traditional method, such as filtration, can not achieve such separation. Moreover, the concentration of bioparticles is generally very low and conventional methods employed for the detection of microorganisms usually require high cell population [4, 5]. Thus, in order to measure bioparticles at concentrations below the sensitivity of the detection system, the sample needs to be filtered first to remove the unwanted bioparticles or impurities that can block or foul the detection system, then followed by a concentration process to improve the sensitivity. The traditional separation methods, such as cen-

\*Corresponding authors (email: dongqing@mme.uwaterloo.ca; yqsun@dlmu.edu.cn)

trifugal separation and filtration, however, are generally time-consuming and labor-intensive and can hardly perform rapid and sensitive analysis. There is an urgent need for the development of rapid bioparticle manipulation methods, especially to separate the wanted particles from a composite sample mixture.

With the rapid development of microfluidic lab-on-chip technology, there is an increasing interest on the development of separation and analytical techniques that can be applied on the microfluidic chip due to its attractive advantages such as small sample volumes and short analysis time, lower cost, greater sensitivity, improved resolution, and portability [6, 7].

Among the various methods for bioparticles manipulation and separation, dielectrophoresis (DEP) is one of the most popular methods [8, 9]. DEP arises from the interaction of a dielectric particle with a spatially non-uniform electric field. Besides the induced translational motion or reorientation of particles by DEP force, there are also several other effects such as traveling wave, quadrupole, and rotational effects.

DEP was discovered by Pohl [10], and its first application with microbes was reported in 1966 [11]. Because electric fields can be scaled down easily on the microfluidic chip, a highly non-uniform electric field at a length scale comparable to particle size can be generated at relatively low voltages. Interesting applications of DEP on bioparticle manipulation on microfluidic chips, such as virus [12, 13], bacteria [14–17], blood cells [18], yeast cell [19, 20], and microalgae [21], have been reported. More details on the environmental application of DEP technique can be found in the review [1].

DC dielectrophoresis (DC-DEP) uses insulating objects, such as obstruction or hurdles made of electrically insulating materials, in a microchannel to create spatial nonuniform electric field required for the dielectrophoresis. DC-DEP system is simple for microfabrication, and has found many applications on bioparticles manipulation [22].

This paper reports a microfluidic method for continuous separation of marine algae and particles by the combination of DC dielectrophoresis and electroosmotic flow. Both the particles and algae are subject to a negative DEP force whose magnitude depends on the volume, shape and dielectric properties of the particles and algae. As a result, the separations of algae of two different sizes, mixture of algae and polystyrene particles with similar volume but different dielectric properties are demonstrated. This is the first application of DC DEP separation of polystyrene particles and algae with similar sizes and illustrates the great influence of dielectric properties on particle separation and potentials for bioanalysis. To the best knowledge of the authors, this is the first report on DC DEP separation of particles by different dielectric properties which is normally achieved by AC-DEP.

## 2 Principle of dielectrophoresis separation

Consider a dielectric particle in an electrically conducting liquid. In the presence of an externally applied electric field, the particles and the surrounding medium are electrically polarized, and the surface charge accumulates at the interfaces due to the difference in electrical permittivity and conductivity of the particle and the liquid. The polarization induces an effective dipole on the particle and the DEP force arises because of the interaction of the particle's dipole and the spatial gradient of the electric field. The DEP force on a particle is given by the following general expression:

$$F_{\text{DEP}} = (\text{volume}) \cdot (\text{polarizability}) \cdot (\text{local electric field}) \cdot (\text{field gradient}) \quad (1)$$

Specifically, for an insulating spherical particle of radius  $a$ , in a nonuniform AC electric field  $E$ , the net DEP force is given by [23, 24]:

$$F_{\text{DEP}} = 2\pi \varepsilon_m a^3 \tilde{f}_{\text{CM}} \nabla |E|^2 \quad (2)$$

where  $\varepsilon_m$  is the electrical permittivity of the suspending medium;  $\tilde{f}_{\text{CM}}$  is the Clausius-Mossotti (CM) factor, which describes the relaxation in the effective polarisability of the particle.

When the frequency is zero (for DC DEP), the CM factor is reduced to [25, 26]:

$$f_{\text{CM}} = \frac{\sigma_p - \sigma_m}{\sigma_p + 2\sigma_m} \quad (3)$$

where  $\sigma_p$  and  $\sigma_m$  are the electrical conductivity of the particle and suspending medium, respectively.

The conductivity for polystyrene particles can be calculated as follows [27]:

$$\sigma_p = \sigma_b + \frac{2ks}{r} \quad (4)$$

where  $\sigma_b$  is the bulk conductivity of the particle,  $\sigma_b = 0$  for polystyrene, and  $ks$  is the general surface conductance, typically 1 nS for polystyrene, and  $r$  is the radius of the particle [28]. Therefore, for the homogeneous 5  $\mu\text{m}$  polystyrene particle, its conductivity is on the order of  $10^{-3}$  S/m, while many buffers are on the order of  $10^{-2}$  S/m [29, 30]. The effective conductivity of most microorganisms is in the range of  $10^{-3}$ – $10^{-4}$  S/m [31].

Figure 1 shows the dependence of CM factor on the conductivity of particles. As can be seen, both polystyrene particles and most microalgae have negative  $f_{\text{CM}}$  values, and thus negative DEP behaviors. Also, microalgae and polystyrene particles have different values of CM factor due to their conductivity differences, which means that it is possi-

ble to separate microalgae and polystyrene particles with similar volume by DC DEP method.

In this paper, electroosmotic flow (EOF) of an electrolyte solution is generated inside the microchannel under an applied DC electric field. The liquid properties are assumed to be uniform throughout the channel. Joule heating effects are neglected [32, 33]. The channel walls are made of electrically insulating materials (PDMS). A triangular PDMS hurdle is fabricated in the middle section. Figure 2 illustrates the electric-field lines and the electric-field strength around the tip of the hurdle. Because the total current is conserved in any cross-section of the channel, the electric field is constricted in the gap region between the hurdle and the channel wall. Thus a stronger and nonuniform local electric field is created near the tip of the hurdle. Since the negative DC-DEP force directs to the local field minimum, the parti-

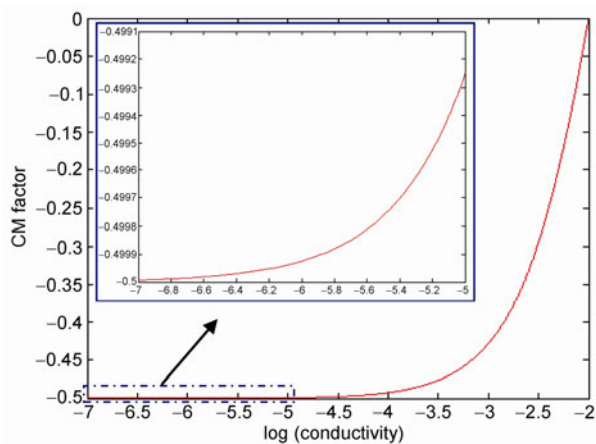


**Figure 1** Dependence of CM factor on the conductivity of particles ( $\sigma_m = 0.01$  S/m).

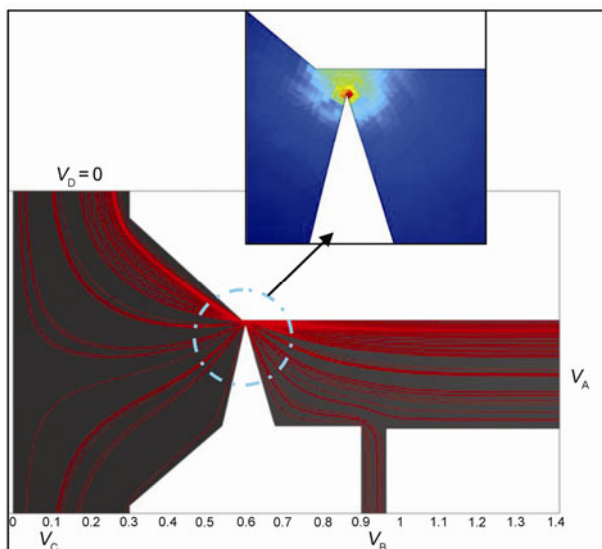


**Figure 2** Distribution of the electric-field lines and the electric-field strength  $E$  around the hurdle. Red color indicates the strongest electric field.  $V_A$ ,  $V_B$ ,  $V_C$  and  $V_D$  are the voltages at each well ( $V_A > V_B > V_C > V_D$ ).

cle experiences a repulsive force when it moves around the tip of the hurdle. The magnitude of the repulsive DEP force is proportional to the particle size and its dielectric properties. Therefore different bioparticles are subjected to different DEP forces and tend to be deflected away to different stream lines. Consequently, the particles can be directed into different collecting wells by controlling the electroosmotic flow streams after the hurdle.

### 3 Experiment

#### 3.1 Chip design

The DC-DEP separation chip and the specific dimension of the microstructure are shown in Figure 3. There are four branches connected to four different wells. Well A and B are for the driving buffer solution and the sample mixture, respectively. Well C and D are for collecting the separated particles. Branches A, C, and D are 300  $\mu\text{m}$  in width. Branch B is 90  $\mu\text{m}$  in width. All of the branch channels are 25  $\mu\text{m}$  in depth. The key structure is a triangular hurdle (240  $\mu\text{m}$  in base width, 130  $\mu\text{m}$  in height) located between the inputting branches (A and B) and the separation branches (C and D). The PDMS (poly-dimethylsiloxane) microchannel was fabricated following the common soft lithography protocol [34].

The voltage applied at electrode A is highest and determines both the overall voltage level of the chip and the throughput of separation. Other than the voltage level  $V_A$ , the voltage output at electrodes B and C is also important for particle separation. The applied voltage at electrode C is for controlling the downstream flow streams and hence the particle motion after the hurdle.

#### 3.2 Sample preparation

The two algae used in the experiment are axenic cultures of

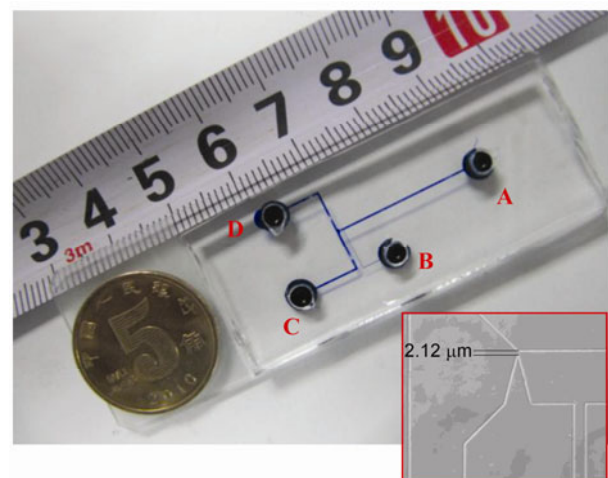


**Figure 3** The DEP separation microfluidic chip used in this study.

*Chlorella vulgaris*, *Pseudokircheriella subcapitata* and *Dunaliella salina* described in the OECD guideline 201. The three types of algae were cultured in 250 mL erlenmeyer flasks containing 60 mL of sterilized f/2 medium and OECD TG201 medium respectively, which were capped with loose cotton. The cultures were kept at  $23 \pm 1$  °C under illumination of approximately  $73.6 \mu\text{mol m}^{-2} \text{s}^{-1}$  on a 16 h light and 8 h dark cycle. The particle used in the experiment is the 5  $\mu\text{m}$  polystyrene particle (79633-F, RS -Fluka). Before the tests, highly concentrated particle samples were diluted greatly and mono-dispersed in sodium borate buffer solution (pH 7.5).

### 3.3 The effective volume measurement of algae

In this study, possible separation of polystyrene particles and algae with similar volume was studied. Because algae do not have a regular shape, it is difficult to determine the volume of algae. The effective volume measurement of algae was achieved by a microfluidic differential resistive pulse (RPS) sensor. Figure 4 shows the working principle of the sensor. Basically, when a particle passes through a narrow gate, the electric resistance of the gate is changed. The measured electric signal is related to the particle's volume. The details of the sensor and measurement protocols can be found in refs. [35, 36].

In order to accurately measure the volume, we use the same microfluidic chip to measure polystyrene particles and the two algae at the same time. Specifically, we first add 5  $\mu\text{m}$  polystyrene particles into the inlet well of the chip and record the RPS signals. Then we remove the polystyrene particle sample from the inlet well and flush the remains in the well with buffer solution to the outlet well. In this way, the polystyrene particle sample can be totally removed from the inlet well. Finally, we add *P. subcapitata* sample and record the signals. For the volume measurement of *D. salina*, we followed the same procedure.

### 3.4 Experimental protocol

Before loading a sample, the microchannels and wells are

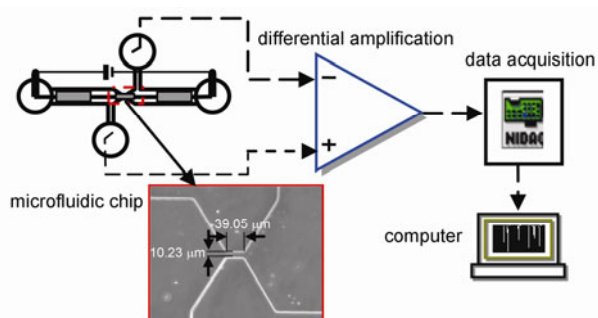


**Figure 4** A schematic diagram of the RPS sensor system for evaluating algae volume.

primed with sodium borate buffer (pH 7.5). Then the cell mixture was introduced into well B with a pipette. A high-voltage DC power supply (Spellman High Voltage Inc., Hauppauge, NY) was used to drive the fluid flow through the microchannel network by platinum electrodes submerged in each well. A custom-made voltage controller was used to adjust individual voltage output of the four electrodes. In the experiments, electrode D was always grounded. The voltage outputs to electrodes A, B, and C were carefully adjusted to ensure that the fluids in the inputting branches A and B always moved towards the hurdle and flowed into the separation branches C and D.

The particle motion was monitored by an inverted optical microscope (Ti-E, Nikon) and recorded by a progressive CCD camera (DS-Qi1Mc, Nikon). The camera was operated in video mode at a frame rate of 11.4 frames per second. The reading error in determining the particle position is about  $\pm 2$  pixels which corresponds to actual dimension of  $\pm 5.4 \mu\text{m}$ .

## 4 Results and discussion

### 4.1 Volume measurement

Figure 5 shows the typical RPS signals of 5  $\mu\text{m}$  polystyrene particles (Figure 5(a)), *P. subcapitata* (Figure 5(b)) and *D. salina* (Figure 5(c)) measured on the same RPS microfluidic chip. Each peak represents one particle/alga and the magnitude is proportional to its volume. As can be seen from the figure, the signal magnitudes of 5  $\mu\text{m}$  polystyrene particles are very uniform due to their uniform sizes. The signals of the two algae, however, are not uniform. To decide the thresholds for *P. subcapitata* and *D. salina*, the RPS signal amplitudes of the two algae and impurity were carefully measured while each was observed by an optical microscope (Nikon Eclips Ti, Nikon, Japan) and the threshold for *P. subcapitata* was set to 2.0 V and 1.8 V for *D. salina*.

According to the theory, the relationship of particle size and its RPS signal magnitude can be calculated as [37]:

$$\frac{V_{\text{out},1}}{V_{\text{out},2}} \approx \left( \frac{d_1}{d_2} \right)^3 \quad (5)$$

where  $V_{\text{out},1}$  is the RPS signal magnitude of particle 1,  $V_{\text{out},2}$  is the RPS signal magnitude of particle 2,  $d_1$  and  $d_2$  are the diameters.

Based on eq. (5) and the signals of 5  $\mu\text{m}$  polystyrene particles, we can get the size distributions of *P. subcapitata* and *D. salina*, as shown in Figure 6. As can be seen from Figure 6, the size distributions of the two algae are scattered heavily and there are big portions of algae whose sizes are larger than 5  $\mu\text{m}$ : about 35% for *P. subcapitata* and 32% for *D. salina*.

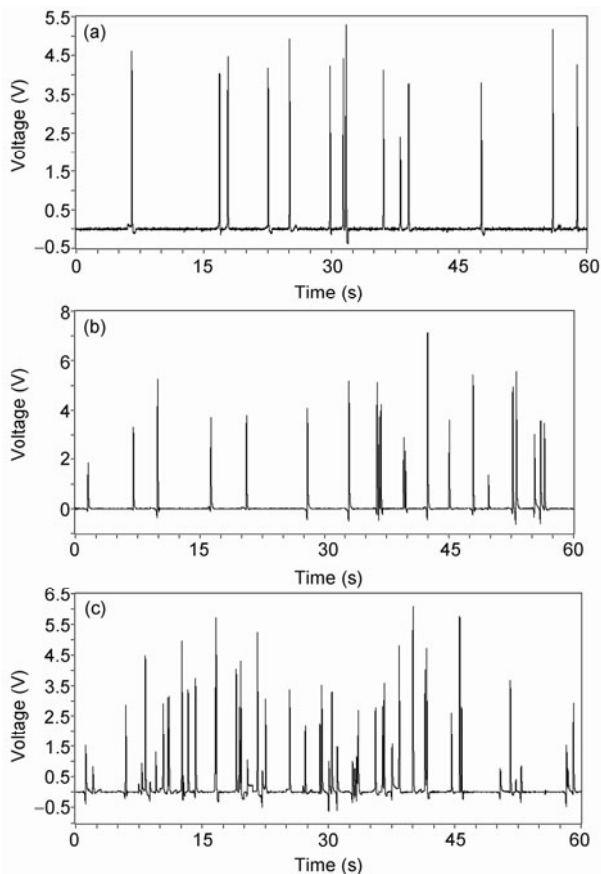


**Figure 5** Typical RPS signals of 5 μm polystyrene particles (a), *P. subcapitata* (b) and *D. salina* (c).

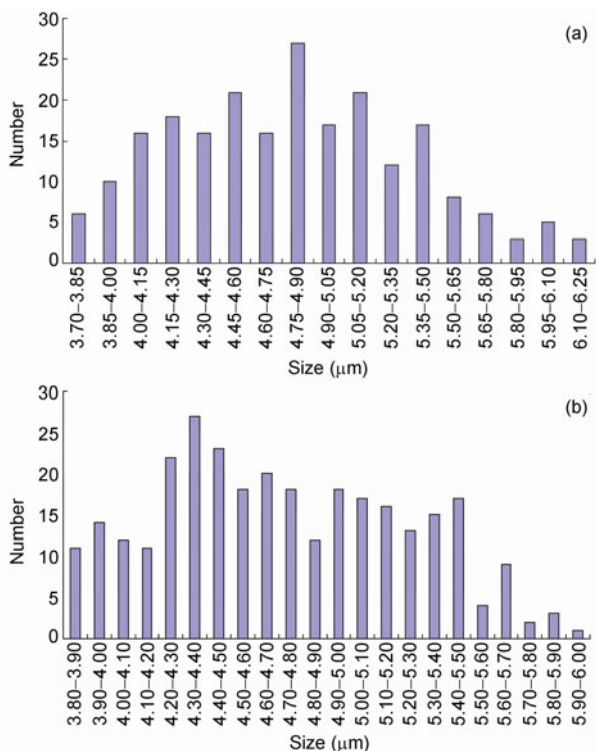


**Figure 6** Size distribution of *P. subcapitata* (a) and *D. salina* (b).

## 4.2 Separation of *C. vulgaris* and *P. subcapitata* by size

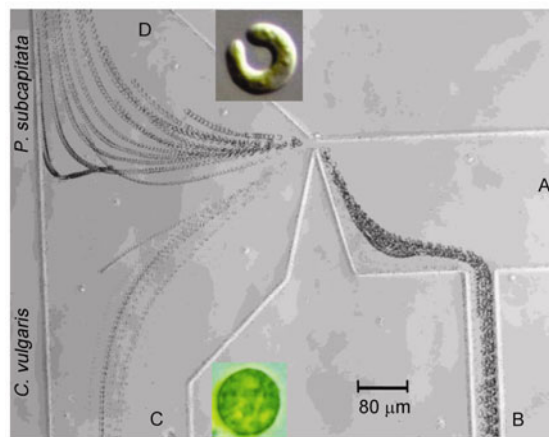
A typical case of separation of *C. vulgaris* and *P. subcapitata* is shown in Figure 7, which is obtained by superposing a series of consecutive images of the moving algae. As can be seen from Figure 7, *C. vulgaris* and *P. subcapitata* are carried down to well C and D, respectively. This can be well explained by the DEP theory.

According to the theory, the magnitude of the alga trajectory deviation is proportional to the DEP force acting on it, and hence its size. Therefore the algae trajectories of different sizes can be repulsed into different streams after they pass the hurdle. Since *C. vulgaris*, around 2–4 μm in diameter, is much smaller than *P. subcapitata*, *P. subcapitata* will be pushed a little far away from the hurdle. Accordingly, the trajectory deviation of *C. vulgaris*, which is less pushed by the hurdle, is smaller due to its small size. By careful adjusting the voltage at electrode A, *P. subcapitata* and *C. vulgaris* can be carried to well D and C by the EOF flow, respectively. Thus the single stream of mixed cells is separated into different streams just simply by adjusting the applied voltages. For *P. subcapitata*, it should be noted that there are more than one trajectory after the hurdle, which is caused by their uneven sizes.

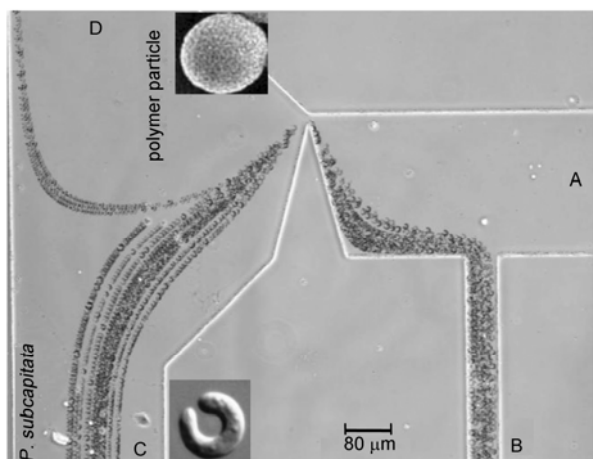
## 4.3 Separation of 5 μm polystyrene particles and algae by dielectric property

Figure 8 shows the separation of 5 μm polystyrene particles and *P. subcapitata*. It's interesting to see that the 5 μm particle, which is smaller in size than some parts of *P. subcapitata*, is directed upwards to well D. On the contrary, all of *P. subcapitata* is carried downwards to well C. As indicated in Figure 6, there are some *P. subcapitata* whose sizes are larger than 5 μm. However, Figure 8 indicates that the smaller polystyrene particle is subject to a bigger negative DEP force than that acting on the *P. subcapitata*.

As indicated by eq. (1), the DEP force is mainly deter-



**Figure 7** DEP separation of *C. vulgaris* and *P. subcapitata* ( $V_A = 295$  V,  $V_B = 117$  V,  $V_C = 17$  V,  $V_D = 0$  V).



**Figure 8** DEP separation of 5  $\mu\text{m}$  polystyrene particles and *P. subcapitata* ( $V_A = 192\text{ V}$ ,  $V_B = 91\text{ V}$ ,  $V_C = 70\text{ V}$ ,  $V_D = 0\text{ V}$ ).

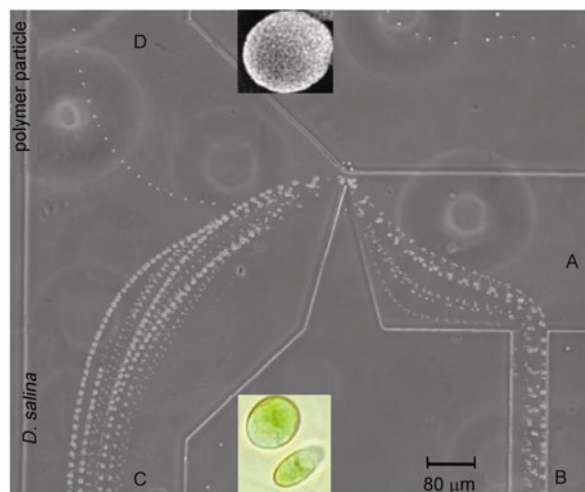


**Figure 9** DEP separation of 5  $\mu\text{m}$  polystyrene particle and *D. salina* ( $V_A = 358\text{ V}$ ,  $V_B = 188\text{ V}$ ,  $V_C = 153\text{ V}$ ,  $V_D = 0\text{ V}$ ).

mined by volume, polarizability (CM factor) and the electric field. *P. subcapitata* is a kind of single-cell alga. As is known, a cell has cytoplasm enclosed by a membrane which, in turn, is surrounded by a cell wall. While the cytoplasm contains a high concentration of ions, the resistance of membrane is so high that can be considered as non-conducting. The cell wall, however, is readily permeable to small molecules and ions and can be regarded as conductive [38]. Also, the polarizability of *P. subcapitata* depends on its composition, morphology, and phenotype [39]. The conductivity of the alga is larger than that of polystyrene particle. As a result, the particle's absolute value of CM factor is larger than that of *P. subcapitata*, which will result in a larger DEP force. In addition, the soft conductive cell wall under the high electric field and the composite composition and structure of the cell might also be the possible causes.

Since alga's morphology will also influence the polarizability, to further investigate whether the irregular form of *P. subcapitata* or its conductivity that cause the decrease of its DEP force, separation of 5  $\mu\text{m}$  polystyrene particle and *D. salina*, which is rod to ovoid shaped (10–12  $\mu\text{m}$  long) with a volume of 50–100  $\mu\text{m}^3$  [40], was performed. Figure 9 shows such a separation.

From Figure 9, it can be seen that the 5  $\mu\text{m}$  polystyrene particle still goes upwards while all of *D. salina*, whose sizes range from 3.8 to 6.0  $\mu\text{m}$ , are directed downward to well C. The repeated separation results also imply that the dielectric difference, not the size difference, between polystyrene particle and alga plays a more importance role in DC-DEP separation. This conclusion is also strongly supported by the fact that we failed to separate *P. subcapitata* and *D. salina* by means of DC-DEP which have similar sizes and dielectric properties but different shapes.

However, it should be noted that some limitations still exist for DC-DEP separation of biparticles. One important limitation is the negative effects caused to live cells by the high electric field and the increased temperatures. While

high electric field is essential for the separation, it can cause stress to cell membrane and temperature increase which might kill the cell. Thus, the chip design parameter, such as the channel length and the size of hurdle, is still needed to minimize the negative effects.

## 5 Conclusion

In this paper, DC-dielectrophoresis separation of two kinds of algae by their sizes, separation of algae and 5  $\mu\text{m}$  polystyrene particle by different dielectric properties were demonstrated. The continual separation was achieved by simultaneously employing electrokinetic transportation and DEP repulsion of particles and algae generated by a DC electric field. Both polystyrene particles and algae are subject to negative DEP forces and repulsed away from the hurdle where the electric field is the maximum. By carefully adjusting the applied voltages at the ends of different branches, the separated particles and algae are carried to different branches by the electroosmotic flow, thus achieving the separation of sample mixtures into two collecting wells.

This separation method can separate not only algae with a size difference of only a few microns, but also be sensitive enough to separate polystyrene particles and algae with similar volume but different dielectric properties which are normally achievable by AC DEP method.

This method is simple and efficient and thus has great potentials in the fields of bioanalysis and sample pretreatment.

*The authors wish to thank the financial support from the Fundamental Research Funds for the Central Universities (2011QN105, 2011ZD014) and the Dalian Science and Technology Foundation (2011J21DW005) to SONG YongXin, National Science & Technology Pillar Program of China in 2010 (2010BAC68B02) and Liaoning Science & Technology Program*

(2007405010) to SUN YeQing and the Natural Sciences and Engineering Research Council of Canada through a research grant to LI DongQing.

- 1 Jesús-Pérez NM, Lapizco-Encinas BH. Dielectrophoretic monitoring of microorganisms in environmental applications. *Electrophoresis*, 2011, 32: 2331–2357
- 2 Klodzinska E, Buszewski B. Electrokinetic detection and characterization of intact microorganisms. *Anal Chem*, 2009, 81: 8–15
- 3 Liu BF, Xu B, Zhang GS, Du W, Luo QM. Micro-separation toward systems biology. *J Chromatogr A*, 2006, 1106:19–28
- 4 Koubova V, Brynda E, Karasova L, Skvor J, Homola J, Dostalek J, Tobiska P, Rosicky J. Detection of foodborne pathogens using surface plasmon resonance biosensors. *Sens Actuator B-Chem*, 2001, 74: 100–105
- 5 Naravani R, Kaiser J. Rapid detection of food-borne pathogens by using molecular techniques. *J Med Microbiol*, 2005, 54: 51–54
- 6 Duffy DC, McDonald JC, Schueller OJA, Whitesides GM. Rapid prototyping of microfluidic systems in poly(dimethylsiloxane). *Anal Chem*, 1998, 70: 4974–4984
- 7 Whitesides GM. The origins and the future of microfluidics. *Nature*, 2006, 442: 368–373
- 8 Gascoyne PRC, Vykoukal J. Particle separation by dielectrophoresis. *Electrophoresis*, 2002, 23: 1973–1983
- 9 Hughes MP. Strategies for dielectrophoretic separation in laboratory-on-a-chip systems. *Electrophoresis*, 23: 2569–2582
- 10 Pohl HA. The motion and precipitation of suspensions in divergent electric fields. *J Appl Phys*, 1951, 22: 869–871
- 11 Pohl HA, Hawk I. Separation of living and dead cells by dielectrophoresis. *Science*, 1966, 152: 647–649
- 12 Morgan H, Hughes MP, Green NG. Separation of submicron bioparticles by dielectrophoresis. *Biophys J*, 1999, 77: 516–525
- 13 Hughes MP, Morgan H, Rixon FJ. Dielectrophoretic manipulation and characterization of herpes simplex virus-1 capsids. *Eur Biophys J Biophys Lett*, 2001, 30: 268–272
- 14 Gadish N, Voldman J. Emergent behavior in particle-laden microfluidic systems informs strategies for improving cell and particle separations. *Anal Chem*, 2006, 78: 7870–7876
- 15 Li H, Bashir R. Dielectrophoretic separation and manipulation of live and heat-treated cells of *Listeria* on microfabricated devices with interdigitated electrodes. *Sens Actuator B-Chem*, 2002, 86: 215–221
- 16 Marx GH, Dyda PA, Pethig R. Dielectrophoretic separation of bacteria using a conductivity gradient. *J Biotechnol*, 1996, 51: 175–180
- 17 Lapizco Encinas BH, Simmons BA, Cummings EB, Fintschenko Y. Insulator-based dielectrophoresis for the selective concentration and separation of live bacteria in water. *Anal Chem*, 2004, 76: 1571–1579
- 18 Kang YJ, Li DQ, Kalams SA, Eid JE. DC-Dielectrophoretic separation of biological cells by size. *Biomed Microdevices*, 2008, 10: 243–249
- 19 Suehiro J, Zhou GB, Imamura M, Hara M. Dielectrophoretic filter for separation and recovery of biological cells in water. *IEEE Trans Ind Appl*, 2003, 39: 1514–1521
- 20 Kang Y, Cetin B, Wu Z, Li D. Continuous particle separation with localized AC-dielectrophoresis using embedded electrodes and an insulating hurdle. *Electrochimica Acta*, 2009, 54: 1715–1720
- 21 Gallo-Villanueva RC, Jesús-Pérez NM, Martínez-López, JI, Pacheco A, Lapizco-Encinas BH. Assessment of microalgae viability employing insulator-based dielectrophoresis. *Microfluid Nanofluid*, 2011, 10: 1305–1315
- 22 Srivastava SK, Gencoglu A, Minerick AR. DC insulator dielectrophoretic applications in microdevice technology: A review. *Anal Bioanal Chem*, 2011, 399: 301–321
- 23 Pohl HA. *Dielectrophoresis*. Cambridge: Cambridge University Press, 1978
- 24 Jones TB. *Electromechanics of Particles*. Cambridge: Cambridge University Press, 1995
- 25 Minerick AR. DC dielectrophoresis in lab-on-a-chip devices. In: Li D ed. *Encyclopedia of Micro- and Nanofluidics*. Berlin: Springer, 2008
- 26 Keshavamurthy SS, Leonard KM, Burgess SC, Minerick AR. Direct current dielectrophoretic characterization of erythrocytes: Positive ABO blood types. In: NSTI-Nanotech, Boston, 2008, 401–404
- 27 Ermolina I, Morgan H. The electrokinetic properties of latex particles: Comparison of electrophoresis and dielectrophoresis. *J Colloid Interface Sci*, 2005, 285: 419–428
- 28 Ozuna-Chacón S, Lapizco-Encinas BH, Rito-Palomares M, Martínez-Chapa SO, Reyes-Betanzo C. Performance characterization of an insulator-based dielectrophoretic microdevice. *Electrophoresis*, 2008, 29: 3115–3122
- 29 Lapizco-Encinas BH, Rito-Palomares M. Dielectrophoresis for the manipulation of nanobiotoparticles. *Electrophoresis*, 2007, 28: 4521–4538
- 30 Barrett LM, Skulan AJ, Singh AK, Cummings EB, Fiechtner GJ. Dielectrophoretic manipulation of particles and cells using insulating ridges in faceted prism microchannels. *Anal Chem*, 2005, 77: 6798–6804
- 31 Marx GH, Huang Y, Zhou XF, Pethig R. Dielectrophoretic characterization and separation of micro-organisms. *Mikrobiologie*, 1994, 140: 585–591
- 32 Xuan X, Xu Bo, Sinton D, Li D. Electroosmosis flow with joule heating effects. *Lab Chip*, 2004, 4: 230–236
- 33 Erickson D, Sinton D, Li D. Joule heating and heat transfer in poly(dimethylsiloxane) microfluidic systems. *Lab Chip*, 2003 3: 141–149
- 34 Xia YN, Whitesides GM. Soft lithography. *Annu Rev Mater Sci*, 1998, 28: 153–184
- 35 Song YX, Zhang HP, Chon CH, Chen S, Pan XX, Li DQ. Counting bacteria on a microfluidic chip. *Anal Chim Acta*, 2010, 681: 82–86
- 36 Song YX, Zhang HP, Chon CH, Pan XX, Li DQ. Nanoparticle detection by microfluidic resistive pulse sensor with a submicron sensing gate and dual detecting channels-two stage differential amplifier. *Sens Actuators B*, 2011, 155: 930–936
- 37 Gregg EC, Steidley KD. Electrical counting and sizing of mammalian cells in suspension: an experimental evaluation. *Biophys J*, 1965, 5: 393–405
- 38 Carstensen EL, JR Cox HA, Mercer WB, Natale LA. Passive electrical properties of microorganisms I. conductivity of *Escherichia coli* AND *Micrococcus lysodeikticus*. *Biophys J*, 1965, 5: 289–300
- 39 Yang J, Huang Y, Wang XB, Becker FF, Gascoyne PR. Cell separation on microfabricated electrodes using dielectrophoretic/gravitational field-flow fractionation. *Anal Chem*, 1999, 71: 911–918
- 40 Ginzbuy M. *Dunaliella*: a green alga adapted to salt. *Adv Botanical Res*, 1987, 14: 93–99